Supplementary Material

Biogeochemical Phosphorus Cycling in Groundwater Ecosystems – Insights from South and Southeast Asian Floodplain and Delta Aquifers

Harald Neidhardt[1]*, Daniel Schoeckle[2], Anna Schleinitz[2], Elisabeth Eiche[3], Zsolt Berner[3], Pham T.K. Tram[4], Vi M. Lan[4], Pham H. Viet[4], Ashis Biswas[5], Santanu Majumder[6], Debashis Chatterjee[7], Yvonne Oelmann[1], Michael Berg[8]

[1]Geoecology, Eberhard Karls University Tübingen, 72070 Tübingen, Germany

[2]Isotope Geochemistry, Eberhard Karls University Tübingen, 72074 Tübingen, Germany

[3]Institute of Applied Geosciences, Karlsruhe Institute of Technology, 76131 Karlsruhe, Germany

[4]Research Centre for Environmental Technology and Sustainable Development (CETASD), Hanoi University of Science, Vietnam National University, Hanoi, Vietnam

[5]Department of Earth and Environmental Sciences, Indian Institute of Science Education and Research Bhopal, Bhopal 462066, India

[6]Groundwater Research Group, Texas A&M University 3115 TAMU College Station Texas, United States

[7]Department of Chemistry, University of Kalyani, Kalyani, 741235 Nadia, West Bengal, India

[8]Eawag, Swiss Federal Institute of Aquatic Science and Technology, 8600 Dübendorf, Switzerland

*harald.neidhardt@uni-tuebingen.de

Table of contents:

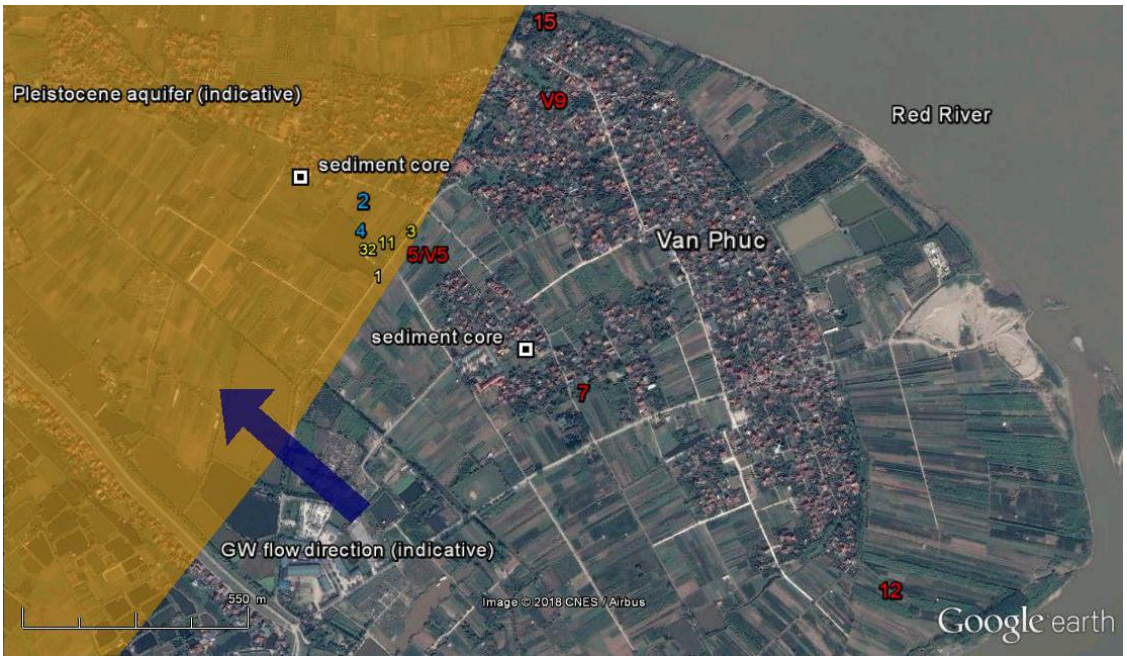

well ID	well depth (m bls)	longitude	latitude
1: AMS-1	25	20°55'15.78"N	105°53'37.98"E
2: AMS-2	25	20°55'22.80"N	105°53'36.96"E
3: AMS-3	25	20°55'19.32"N	105°53'40.44"E
4: AMS-4	38	20°55'19.38"N	105°53'36.17"E
5: AMS-5	24	20°55'17.47"N	105°53'41.82"E
7: AMS-7	38	20°55'06.53"N	105°53'55.00"E
11: AMS-11	25	20°55'18.42"N	105°53'38.34"E
12: AMS-12	25	20°54'50.95"N	105°54'20.94"E
15: AMS-15	28	20°55'35.84"N	105°53'51.68"E
32: AMS-32	25	20°55'18.69"N	105°53'37.53"E
V5 : VPNS-5	31	20°55'17.47"N	105°53'41.82"E
V9: VPNS-9	26	20°55'29.60"N	105°53'52.48"E
Red River	0	20°55'37.48"N	105°53'52.42"E

Fig S1: Investigation area at Van Phuc, which is situated about 30 km south of Hanoi. Monitoring wells in blue indicate groundwater with low TDP concentrations delivered from the Pleistocene aquifer, yellow wells depict groundwater with elevated TDP concentrations from the Pleistocene aquifer adjacent to the Holocene aquifer (referred to as 'transition zone'), and red wells show groundwater from the Holocene aquifer that is characterized by increased TDP concentrations. Due to extensive groundwater withdrawal in the vicinity of Hanoi, the local groundwater flow has been redirected in NW direction. Two sediment cores were collected from the Pleistocene and the Holocene aquifer as indicated in the figure. The study area can be subdivided into the following three distinctive zones: (i) Holocene aquifer sediments with elevated concentrations of TDP in groundwater stretching from the shore of the Red River in the East in direction of wells AMS-5 and VPNS-5 (5/V5) to the West; (ii) Pleistocene aquifer sediments with very low TDP concentrations in groundwater as indicated by the orange colored area, (iii) and the transition zone in between, where groundwater in the Pleistocene aquifer is characterized by constantly high TDP concentrations (see yellow labelled wells AMS-1, -3, -11 and -32 to the West). Highest concentrations of TDP occur within a plume in depths of about 20 to 40 m below ground surface. Groundwater zonation after Al Lawati et al. (2012), van Geen et al. (2013) and Weinman et al. (2008).

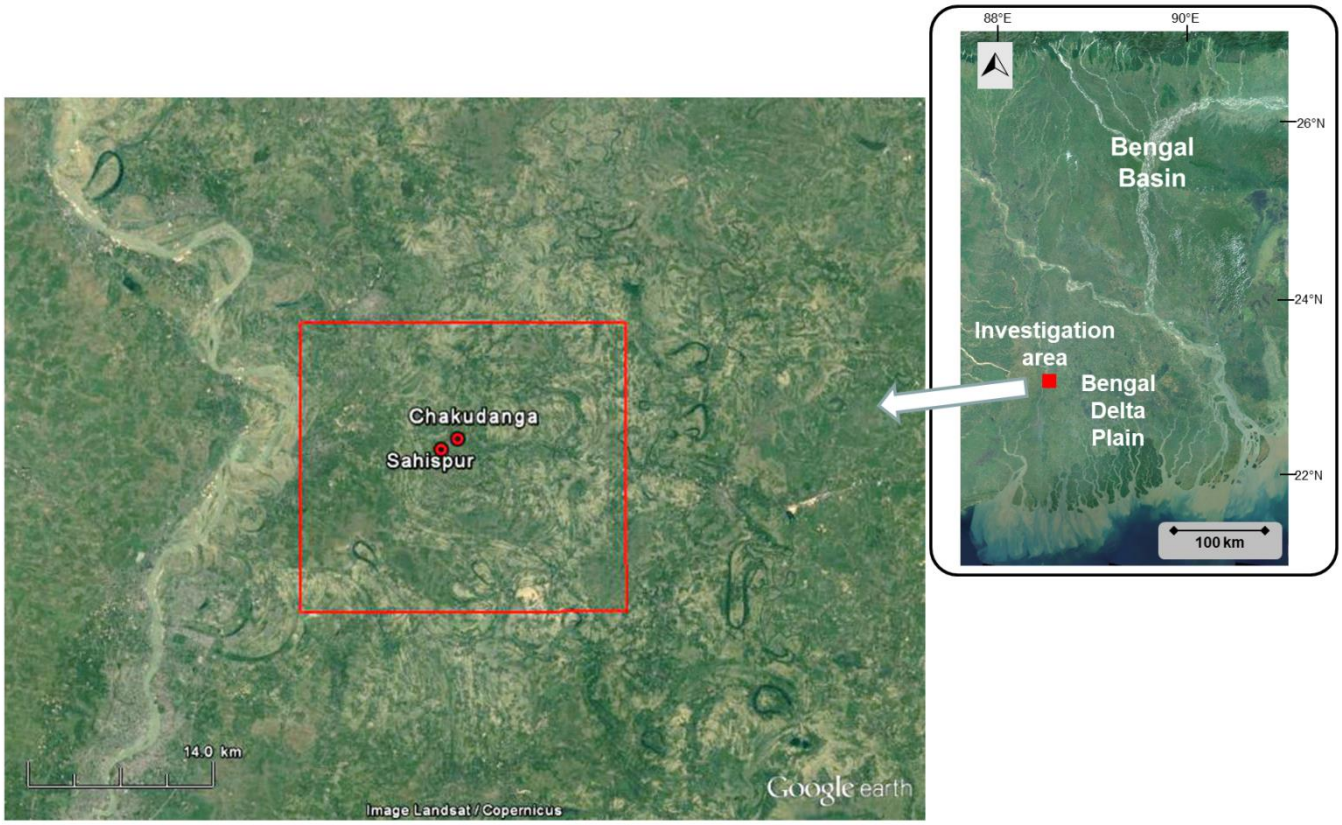

Fig. S2: Satellite image illustrating the location of our study area and the two study sites (Chakudanga and Sahispur) within the Nadia District of the BDP. Red lines indicate the sampling area of the preliminary groundwater survey, which covered an area of 20 x 20 km^2.

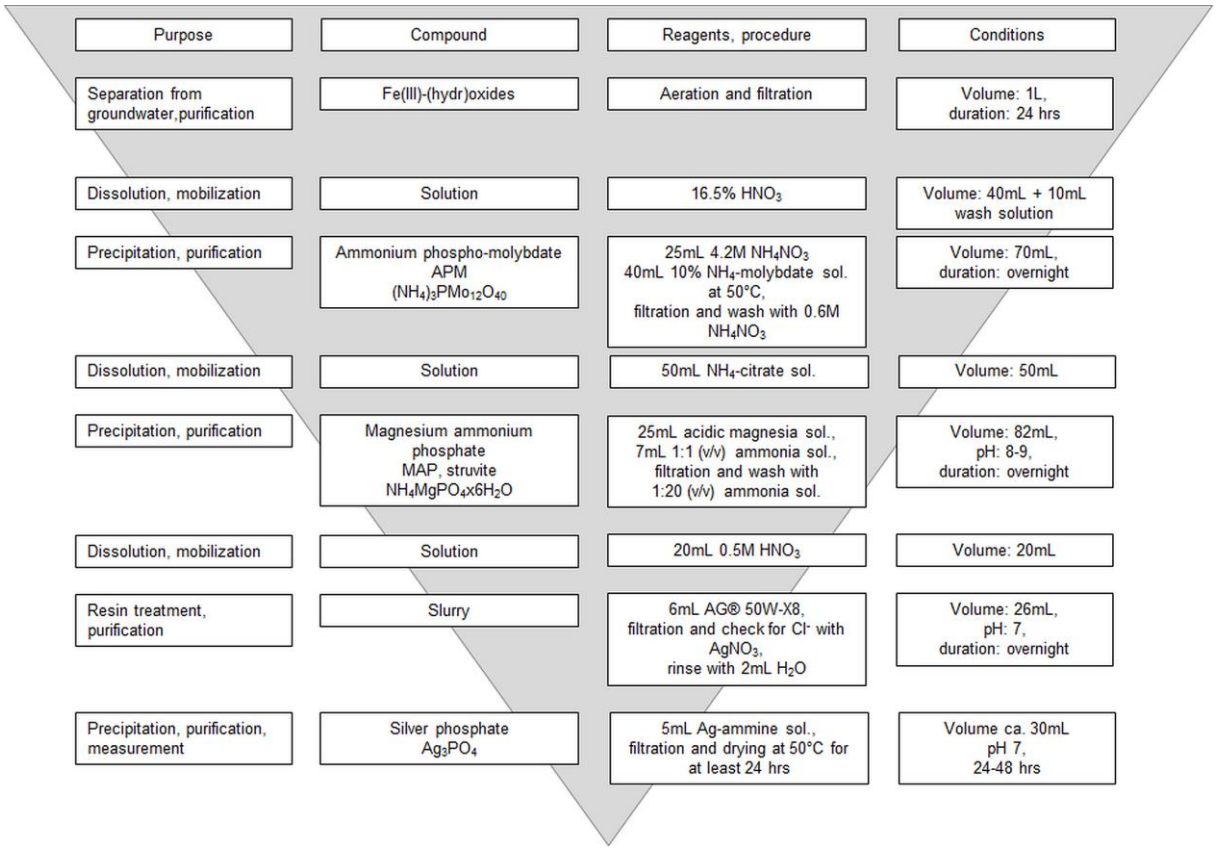

Fig. S3: Modified analytical protocol for the separation, pre-concentration and purification of inorganic P obtained from anoxic groundwater prior to the analysis for $\delta^{18}O_{PO4}$ by IRMS after Gruau et al. (2005), McLaughlin et al. (2004) and Tamburini et al. (2010).

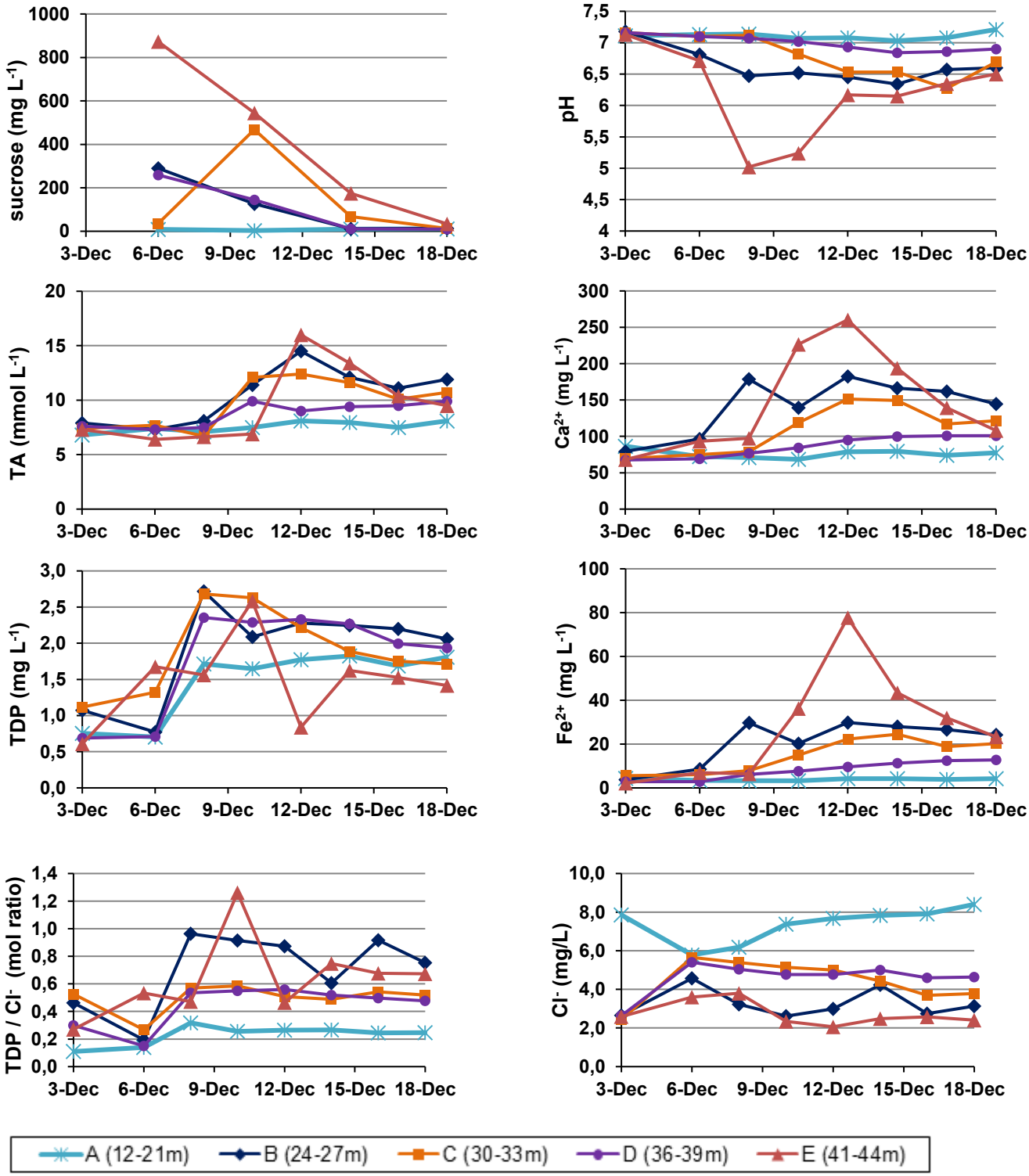

Fig. S4a: Short-term response of groundwater of the nested monitoring wells A to E in Chakudanga (BDP) to the *in situ* biostimulation experiment. Sucrose was added on 4th and 5th Dec. 2009. Note: an increase of TDP occurred not only in the four sucrose infused wells (B to E), but also in groundwater of the shallowest well A (screened between 12-21 m bls). Furthermore, the increase in TDP predates those in Fe^{2+} and Ca^{2+}. Data from Neidhardt et al. (2014), except for TDP.

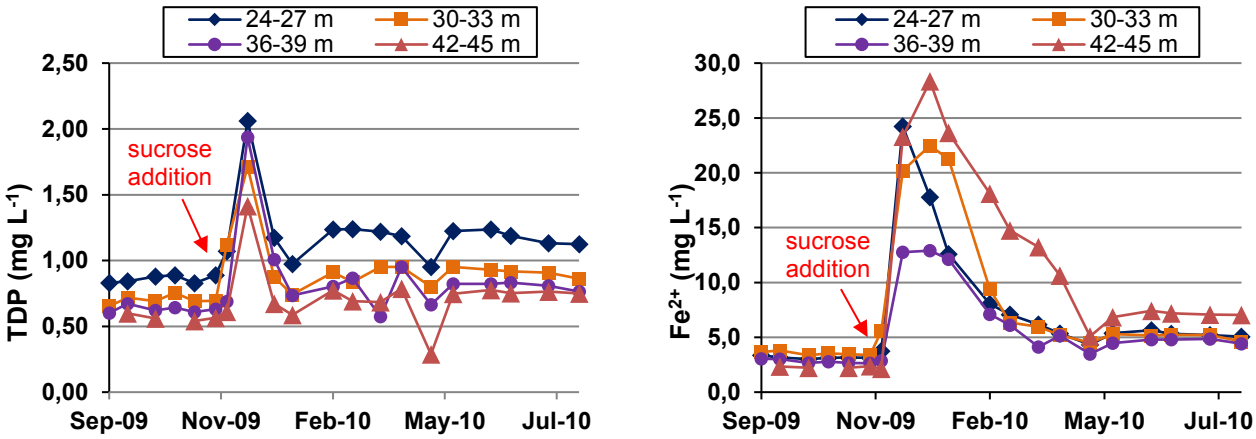

82

well	screening	TDP baseline (mg L^{-1}), Dec 2009	TDP (mg L^{-1}) max, d after sucrose addition	TDP (mg L^{-1}) end of monitoring, Aug 2010	% change*
well A	12-21	0.75	1.82 (10d)	0.79	+5
well B	24-27	1.07	2.72 (4d)	1.12	+5
well C	30-33	1.12	2.68 (4d)	0.86	-23
well D	36-39	0.69	2.36 (4d)	0.76	+10
well E	41-44	0.61	2.58 (6d)	0.75	+23

83 *baseline before the experiment (Dec. 2009) vs end of monitoring (Aug. 2010)

84 **Fig. S4b:** Long-term response of groundwater in the four sucrose amended-wells B to E to the *in situ*
85 biostimulation experiment. Note: while TDP concentrations declined rapidly, initial baseline concentrations
86 predating the experiment were not fully met in three out of the four wells. Data from Neidhardt et al. (2014) and
87 Biswas et al. (2014).

88

89

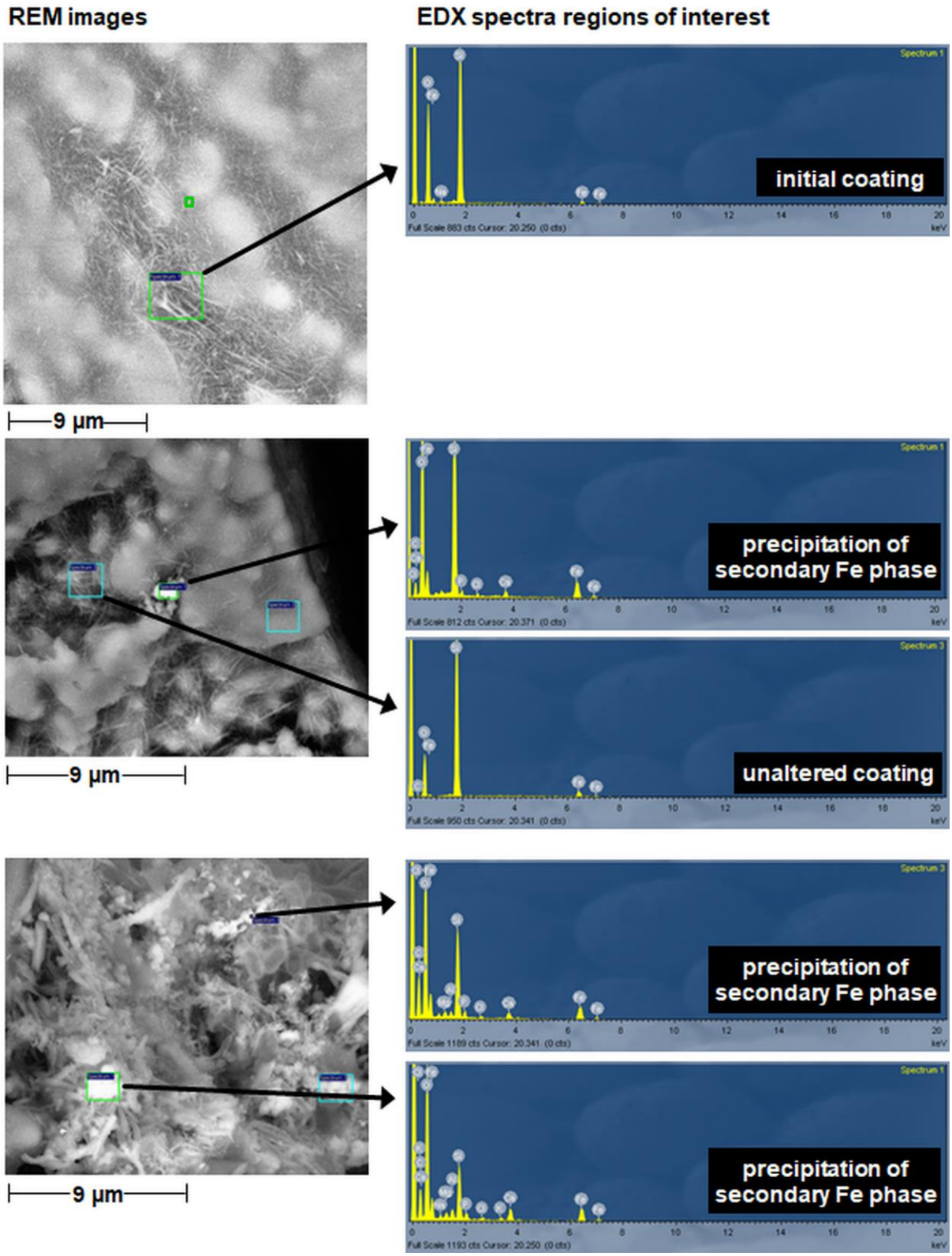
REM images
EDX spectra regions of interest
initial coating
9 µm
precipitation of secondary Fe phase
unaltered coating
9 µm
precipitation of secondary Fe phase
precipitation of secondary Fe phase
9 µm

90

Fig. S5: Scanning electron microscope (SEM) images and coupled energy-dispersive X-ray spectroscopy (EDX) spectra of goethite-coated sand samples. Top: initial coating of sub-micrometer goethite needles before the *in situ* exposure experiments. Mid: sample surface after six months exposure to reducing groundwater of well AMS-1 (E_h: +45 mV), including precipitation of cubic Fe-minerals that contained traces of P and Ca (see corresponding EDX spectrum 1). Bottom: formation of secondary minerals after one week exposure to groundwater of well AMS-1. The newly formed cubic mineral aggregates contained traces of P, Ca, Mg, K, Al, Na and Cl in additon to Fe and O (see EDX spectrua 1 & 3). Reprinted from Neidhardt et al. (2018), permission for reproduction granted from Elsevier.

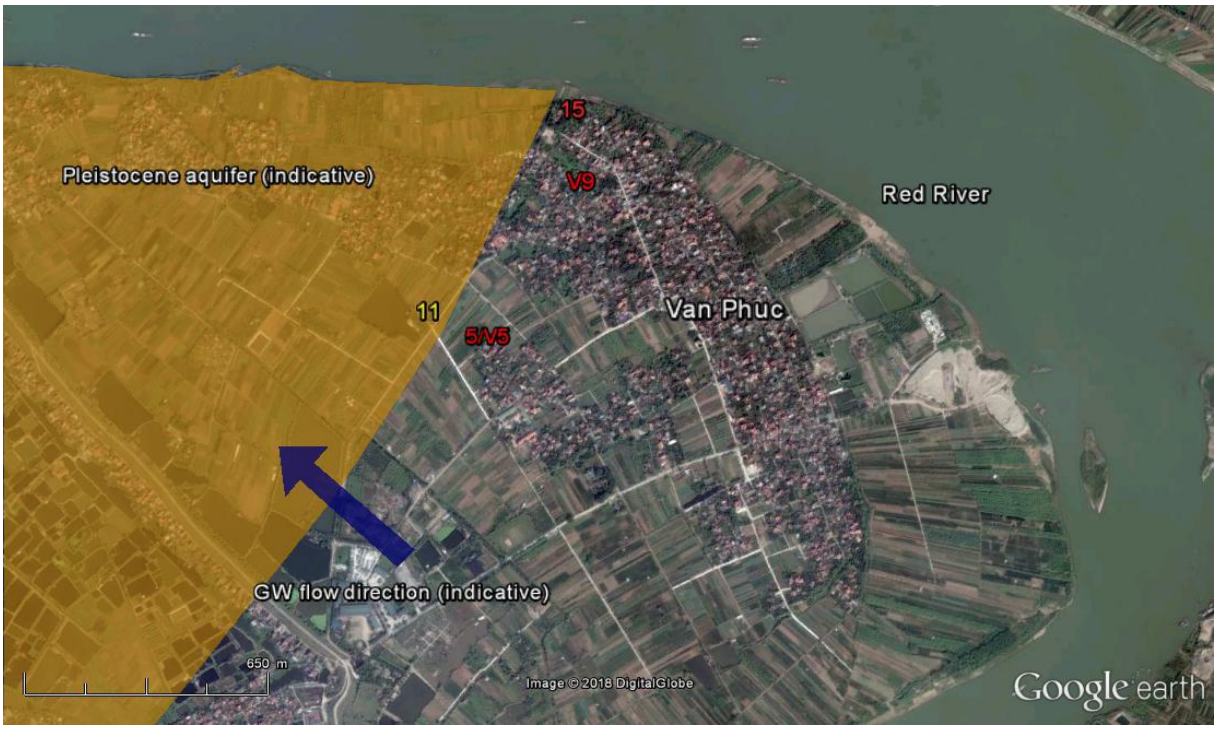

Well ID (screening m bls)	TDP (mg L^{-1})	$\delta^{18}O_{PO4}$ (‰ VSMOW) measured	T (°C)	$\delta^{18}O_{H2O}$ (‰ VSMOW)	$\delta^{18}O_{PO4}$ expected equilibrium (Longinelli and Nuti 1973)	$\delta^{18}O_{PO4}$ expected equilibrium (Chang and Blake 2015)	$\Delta_{sample-equil}$ (Chang & Blake 2015)
5: AMS-5 (23-24)	1.30	+15.42 ± 0.06	26.7	-7.06	+12.64	+14.61	0.81
V5: VPNS-5 (30-31)	0.73	+14.60 ± 0.09	26.3	-7.64	+12.16	+14.08	0.52
V9: VPNS-9 (25-26)	1.50	+16.78 ± 0.29	25.3	-6.55	+13.48	+15.36	1.42
11: AMS-11 (24-25)	0.26	+15.02 ± 0.31	26.6	-6.63	+13.10	+15.07	-0.04
15: AMS-15 (27-28)	0.03	[1)]	25.6	-7.26	+12.69	+14.58	

Fig. S6: Sampled wells in the investigated area and their $\delta^{18}O_{PO4}$ isotopic composition. Included are also screening positions, TDP concentrations, $\delta^{18}O_{H2O}$ values and water temperature (T) of the groundwater samples. In addition, expected equilibrium values (after Chang and Blake (2015)) and deviations (Δ) of measured $\delta^{18}O_{PO4}$ values from respective expected equilibrium values are shown. The satellite image depicts the well locations and the approximate positions of the Holocene and Pleistocene aquifer as well as the groundwater flow direction (indicative). The $\delta^{18}O_{PO4}$ values covered a range of >2‰ and mostly deviate notably from the expected equilibrium value. [1)]well AMS-15 did not yield sufficient Ag_3PO_4 for the $\delta^{18}O_{PO4}$ analysis

Table S1: Absolute and relative removal efficiency for TDP and DOC by co-precipitation of Fe-(hydr)oxides formed by aeration of fresh groundwater samples (1 L per sample, respectively). Contents determined from concentration differences in water samples before and after aeration.

well ID	TDP		Fe^{2+}		DOC	
	mg	%	mg	%	mg	%
2015						
AMS-5	1.30	100	10.7	100	0.33	3.7
VPNS-5	0.73	100	12.6	100	0.41	20.2
AMS-7	1.03	100	6.13	100	0.31	11.4
VPNS-9	1.50	100	16.1	100	0.91	43.7
AMS-11	0.26	100	10.1	100	0.22	7.6
AMS-12	0.25	100	6.57	100	3.89	84.1
AMS-15	0.03	100	0.71	100	0.14	12.0
AMS-32	0.51	100	7.59	100	0.03	1.8
2013						
AMS-5	1.69	87.1	13.0	87.6	nd	nd
VPNS-5	0.76	100	13.9	99.8	nd	nd
AMS-7	1.02	97.9	6.36	99.7	nd	nd
VPNS-9	1.46	99.7	11.7	99.9	nd	nd
AMS-11	0.77	100	11.3	99.8	nd	nd
AMS-12	0.98	100	13.3	99.9	nd	nd
AMS-15	0.05	100	1.14	99.3	nd	nd
AMS-32	0.88	99.2	8.58	98.7	nd	nd

nd: not determined

Table S2: Bulk TP and Fe contents in sediments of the field sites and TDP concentrations in groundwater from corresponding depth intervals. Note that a clayey and silty aquitard of around 3 m thickness confines the shallow aquifer towards the surface at the two BDP sites Chakudanga and Sahispur. A similar aquitard of clayey and mainly silty fine deposits reaches down to approximately 23 and 10 m bls, respectively, at the Pleistocene and Holocene aquifer sites at Van Phuc. Sediment and water samples were collected at Van Phuc as described in Eiche et al. (2008), for the two West Bengal sites refer to Neidhardt et al. (2013) and Neidhardt et al. (2014). *Significant correlation ($p < 0.05$).

depth sediment (m bls)	TP sediment (mg kg^{-1})	Fe sediment (g kg^{-1})	well screen (m bls)	TDP groundwater (mg L^{-1})
Van Phuc, Pleistocene aquifer				
0.4	284	58		
3.1	262	68		
4.1	153	30		
7.3	240	45		
8	131	67		
10.8	109	32		
13.8	43.6	29		
15.1	153	62		
18.6	87.3	25		
21.9	109	46		
23.7	109	16	23-24	0.03
27.6	65.5	13	26-27	0.03
32.5	65.5	20	32-33	0.03
38.8	65.5	17	38-39	0.01
47.3	109	32	44-45	0.02
	$r_{s\ Fe,\ P}$: 0.76*			
Van Phuc, Holocene aquifer				
2.8	262	63		
4.1	218	48		
6.3	284	63		
8.7	262	54		
10.9	305	59		
13.2	109	26		
13.6	262	59		
14.7	109	29		
16.6	240	53	16-17	0.69
20.8	109	22	20-21	0.62
27.3	109	23	26-27	0.20
29.8	65.5	5		
32	87.3	19	33-34	0.18
36.1	43.6	11	35-36	0.39
38.2	43.6	11		
41.6	109	19	40-41	0.46
44.1	65.5	15	44-45	0.37
46.8*	87.3	20		
49.3*	65.5	17		
53.6*	65.5	20	56-57	0.16
	$r_{s\ Fe,\ P}$: 0.94*			

depth sediment	TP sediment	Fe sediment	well screen	TDP groundwater
Nadia District, Chakudanga				
13	418	16	12-21	0.75
20.1	432	12	12-21	0.75
25.3	337	14	24-27	1.07
30.5	386	17	30-33	0.35
38.3	234	10	36-39	0.69
45.5	371	15	42-45	0.61
	$r_{s\ Fe,\ P}$: 0.37			
Nadia District, Sahispur				
12.4	620	20	12-21	0.83
23.5	223	10	22-25	0.95
29.4	304	15	26-29	0.80
30.7	375	16	30-33	0.97
30.7	354	16	30-33	0.97
38.5	507	37	34-37	0.90
	$r_{s\ Fe,\ P}$: 0.93*			

121

122

Table S3: Saturation indices (SI) computed with PHREEQC for mineral phases that might serve as sink or source for PO_4^{3-}. Values <-0.25 indicate undersaturation, which means dissolution is thermodynamically possible (i.e., amorphous Fe-hydroxides). Values >+0.25 indicate supersaturation, indicating that these minerals remain stable under the prevailing conditions if already present, or might freshly precipitate. Values between -0.25 and +0.25 are considered close to equilibrium, meaning that both, dissolution and precipitation, are considered unlikely. Respective SI values were calculated for water samples taken in Van Phuc in April 2014 (except for AMS-1 and AMS-3, here October 2013), and at Sahispur and Chakudanga (October 2012). Water data originating from Neidhardt et al. (2018), Neidhardt et al. (2014) and Neidhardt et al. (2013). Redox assumptions for Chakudanga O_2: 0.24 mg L^{-1}, Eh: -86 mV, and for Sahispur O_2: 0.24 mg L^{-1}, Eh: -59 mV.

well ID	amorph. Fe-hydroxide	goethite	hematite	magnetite	siderite	vivianite	hydroxy-apatite	strengite	
	$Fe_3(OH)_8$	FeO(OH)	Fe_2O_3	Fe_3O_4	$FeCO_3$	$Fe_3(PO_4)_2 \cdot 8H_2O$	$Ca_5(PO_4)_3OH$	$FePO_4 \cdot 2H_2O$	$MnHPO_4$
Van Phuc									
AMS-1	-3.97	4.50	11.0	12.6	1.10	1.56	-0.55	-1.34	1.82
AMS-2	-3.14	5.60	13.2	13.5	-0.61	-6.15	-4.58	-2.01	0.76
AMS-3	0.09	5.95	13.9	16.7	1.78	2.98	1.85	-0.93	1.81
AMS-4	-3.25	5.58	13.2	13.4	-0.58	-5.34	-1.92	-1.55	1.63
AMS-5	-3.02	4.90	11.8	13.6	1.33	2.40	0.87	-0.71	1.85
AMS-11	-2.17	5.10	12.2	14.4	1.41	2.25	1.25	-1.27	1.70
AMS-12	-2.49	5.02	12.1	14.2	1.38	2.44	2.02	-1.12	2.44
AMS-15	-2.59	5.48	13.0	14.0	0.10	-2.66	-5.32	-1.53	1.67
AMS-32	-2.10	5.09	12.2	14.5	1.37	2.33	1.98	-1.38	3.07
VPNS-5	-1.66	5.31	12.6	14.8	1.46	2.37	1.33	-1.02	1.50
BDP, West Bengal									
Chakudanga									
A (12-21m*)	-5.58	3.51	9.05	11.2	1.01	1.70	2.00	-2.93	2.48
B (22-25m)	-5.29	3.63	9.29	11.4	1.06	1.96	2.66	-2.76	2.44
C (26-29m)	-4.90	3.75	9.51	11.8	1.19	2.50	2.36	-2.58	2.40
D (30-33m)	-5.79	3.44	8.89	10.9	0.91	1.24	1.70	-3.08	2.21
E (34-37m)	-6.36	3.25	8.52	10.4	0.75	0.72	1.46	-3.27	2.32
Sahispur									
A (12-21m)	-5.81	3.44	8.88	10.7	1.11	1.65	1.50	-2.66	2.41
B (24-27m)	-5.73	3.46	8.92	10.8	1.17	1.88	1.68	-2.57	2.37
C (30-33m)	-5.63	3.60	9.22	10.9	0.54	0.16	2.67	-2.99	2.55
D (36-39m)	-4.76	3.85	9.71	11.7	1.06	1.84	2.49	-2.47	2.22
E (42-45m)	-5.54	3.56	9.12	11.0	0.98	1.57	1.60	-2.61	2.28

Table S4: Temporal variation of TDP and Fe^{2+} concentrations in groundwater samples of Van Phuc. TDP concentrations in the majority of the wells remained constant, except for well AMS-5. In addition, TDP concentrations sharply dropped along with Fe^{2+} in water samples collected from four wells (AMS-11, AMS-12, AMS-15 and AMS-32) during the last sampling campaign in April 2015. We attributed this sharp decline to an unusually dry year in 2015, which resulted in a drop-off in the water level and a subsequent aeration of the upper aquifer sediments, probably causing precipitation of Fe(III)-(hydr)oxides and a concomitant removal of Fe^{2+} and PO_4^{3-} from groundwater

well ID	Sampling date	TDP (mg L^{-1})	Fe^{2+} (mg L^{-1})
AMS-1	Oct 2013	0.84	10.0
	Apr 2013	0.59	13.8
	Dec 2009	0.99	16.2
AMS-2	Apr 2015	0.03	0.07
	Apr 2014	0.03	0.12
	Oct 2013	0.02	0.06
	Apr 2013	0.04	0.19
	Dec 2009	0.01	0.36
AMS-4	Apr 2015	0.06	0.13
	Apr 2014	0.10	0.12
	Apr 2006	0.03	0.03
AMS-5	Apr 2015	1.30	10.7
	Apr 2014	1.69	13.2
	Oct 2013	1.94	14.8
	Apr 2013	1.00	8.84
	Dec 2009	2.02	14.2
VPNS-5	Apr 2015	0.73	12.6
	Apr 2014	0.69	13.3
	Oct 2013	0.76	13.9
	Apr 2006	0.83	15.2
AMS-7	Apr 2015	1.03	6.13
	Oct 2013	1.04	6.38
	Dec 2009	1.27	6.92
AMS-11	Apr 2015	0.26	10.1
	Apr 2014	0.70	10.8
	Oct 2013	0.77	11.3
	Apr 2010	0.69	10.0
AMS-12	Apr 2015	0.25	6.57
	Apr 2014	1.02	11.6
	Oct 2013	0.98	13.3
	Apr 2013	0.91	12.6
	Apr 2010	1.00	11.6
AMS-15	Apr 2015	0.03	0.71
	Apr 2014	0.07	1.01
	Oct 2013	0.05	1.15
	Apr 2010	0.08	0.77
AMS-32	Apr 2015	0.51	7.59
	Apr 2014	0.78	8.23
	Oct 2013	0.89	8.69

Table S5: Total P and Fe contents of the adsorption experiment samples, corresponding TDP concentrations and E_h values in groundwater when samples were introduced into the monitoring wells at the Van Phuc study site. Further experimental details provided in the method description. Fe contents and E_h values adopted from Neidhardt et al. (2018).

Well ID	Introduction	Exposure time (days)	TP mg kg^{-1}	±	Fe mg kg^{-1}	±	TDP mg L^{-1}	E_h (mV)
Ferrihydrite-coated sand								
initial	Apr 13	0	<0.32		851	13	0.00	
AMS-1	Apr 13	7	8.60	0.16	632	2	0.59	+45
AMS-5	Apr 13	7	14.2	0.7	578	23	1.00	+29
AMS-12	Apr 13	7	11.2	1.2	589	117	0.90	+19
AMS-1	Oct 13	28	0.37	-	33	11	0.84	+23
AMS-5	Oct 13	28	12.7	0.6	292	7	1.93	+29
VPNS-5	Oct 13	28	4.65	0.86	539	579	0.76	+3
AMS-15	Oct 13	28	<0.32		74	8	0.05	+118
AMS-32	Oct 13	28	6.97	1.81	162	3	0.89	-5
AMS-1	Oct 13	182	<0.32		<0.18	6	0.59	+23
AMS-12	Oct 13	182	<0.32		53	1	0.90	+9
Goethite-coated sand								
initial	Apr 13	0	<0.32		1300	30	0.00	
AMS-1	Apr 13	7	5.34	0.35	1230	6	0.59	+45
AMS-5	Apr 13	7	8.21	1.99	1440	166	1.00	+29
AMS-12	Apr 13	7	4.22	0.41	1220	9	0.90	+19
AMS-1	Oct 13	28	5.09	0.02	1230	25	0.84	+23
AMS-5	Oct 13	28	5.10	1.08	1270	1	1.93	+29
VPNS-5	Oct 13	28	4.89	0.27	1220	16	0.76	+3
AMS-15	Oct 13	28	2.63	0.38	1190	40	0.05	+118
AMS-32	Oct 13	28	6.45	1.75	1260	5	0.89	-5
AMS-1	Oct 13	182	6.06	1.00	1250	22	0.59	+23
AMS-12	Oct 13	182	6.98	1.02	1540	249	0.90	+9
Hematite-coated sand								
initial	Apr 13	0	<0.32		6080	107	0.00	
AMS-1	Apr 13	7	12.2	1.2	6130	820	0.59	+45
AMS-5	Apr 13	7	12.9	0.3	5650	27	1.00	+29
AMS-12	Apr 13	7	14.1	1.0	5830	40	0.90	+19
AMS-1	Oct 13	28	12.4	3.1	5940	395	0.84	+23
AMS-5	Oct 13	28	13.1	1.0	6080	217	1.93	+29
VPNS-5	Oct 13	28	11.4	0.2	5930	91	0.76	+3
AMS-15	Oct 13	28	4.95	0.45	5490	11	0.05	+118
AMS-32	Oct 13	28	12.3	0.5	5920	262	0.89	-5
AMS-1	Oct 13	182	12.5	0.5	5980	190	0.59	+23
Pleistocene sediment								
initial	Apr 13	0	28.1	5.4	2540	408	0.03**	
AMS-1	Apr 13	7	30.5	5.0	2430	276	0.59	+45
AMS-5	Apr 13	7	25.1	0.5	2280	220	1.00	+29
AMS-12	Apr 13	7	26.8	3.1	2490	277	0.90	+19
AMS-1	Oct 13	28	33.3	5.4	2910	534	0.84	+23

AMS-5	Oct 13	28	40.4	0.9	3210	190	1.93	+29
VPNS-5	Oct 13	28	42.3	3.4	3790	92	0.76	+3
AMS-15	Oct 13	28	31.8	3.1	2970	458	0.05	+118
AMS-32	Oct 13	28	31.3	2.6	2960	651	0.89	-5
AMS-1	Oct 13	182	30.7	3.5	2600	448	0.59	+23
AMS-5	Oct 13	182	29.1	4.3	2740	874	1.00	+29
AMS-12	Oct 13	182	26.4	1.6	2690	308	0.90	+9

144

Table S6: Measurement results for $\delta^{18}O_{PO4}$ analysis of Ag_3PO_4 precipitates. Each groundwater sample (except for VPNS-9) was taken and measured as sample duplicate, of which each was analyzed in replicates depending on the available amount of Ag_3PO_4 precipitate. In the lower part, values for the laboratory standard (KH_2PO_4, Roth p.a.) are provided, including processed and directly precipitated samples.

Sample ID	$\delta^{18}O_{PO4}$	avg.	±	n	avg.	±
1. AMS-5a	15.40	15.38	0.14	3	15.42	0.06
	15.51					
	15.24					
2. AMS-5b	15.21	15.46	0.22	3		
	15.64					
	15.54					
1. AMS-11a	15.03	15.24	0.30	2	15.02	0.31
	15.45					
2. AMS-11b	14.90	14.80	0.25	3		
	14.99					
	14.52					
1. VPNS-5a	14.74	14.67	0.10	2	14.60	0.09
	14.60					
2. VPNS-5b	14.47	14.54	0.10	2		
	14.61					
1. VPNS-9a	16.58	16.78	0.29	2	16.78	0.29
	16.98					
1. KH_2PO_4 a	13.01	13.14	0.19	2	13.51	0.35
	13.28					
2. KH_2PO_4b	13.73	13.53	0.17	3		
	13.46					
	13.40					
3. KH_2PO_4c	14.08	13.85	0.25	3		
	13.88					
	13.59					
KH_2PO_4 (pure, unprocessed)	13.50	13.79	0.25	8	13.79	0.25
	14.09					
	13.78					
	13.73					
	14.02					
	14.10					
	13.53					
	13.57					

Table S7: Average TP amounts in solutions and supernatants (top part) and in final Ag_3PO_4 precipitates (middle part) during different steps of sample preparation (determined by ICP-OES). For the respective steps when samples were collected refer to the flow chart presented in Fig. S3 and the detailed method description in the SI. Samples were processed in duplicates, while the internal laboratory control standard (KH_2PO_4, initial TP content: 5 mg) was processed as triplicate. The last part of the table shows the possible influence of a contamination of Ag_3PO_4 with Ag_3AsO_4 on the measured $\delta^{18}O_{PO4}$ values, calculated according to equations S1 and S2. Positive deviations $\Delta_{true\text{-}meas}$ [‰] indicated a higher "true" $\delta^{18}O_{PO4}$ value as if no As was present in the final precipitates (refer to the discussion in the SI for further details).

Sample ID	AMS-5	AMS-11	AMS-15	VPNS-5	VPNS-9	KH_2PO_4*
TP in solution (mg):						
(1) after AMP precipitation	<LOQ	<LOQ	<LOQ	<LOQ	<LOQ	<LOQ
(2) after struvite precipitation	<LOQ	<LOQ	<LOQ	<LOQ	<LOQ	<LOQ
(3) after $AgNO_3$ addition	1.58 ± 0.10	0.59 ± 0.01	0.04 ± 0.00	0.72 ± 0.01	1.41 ± 0.03	4.54 ± 0.13
(4) after AgCl prec. & filtration	1.69 ± 0.33	0.59 ± 0.00	<dl	0.76 ± 0.04	1.48 ± 0.11	4.87 ± 0.41
(5) after final Ag_3PO_4 precipitation	<LOQ	<LOQ	<LOQ	<LOQ	<LOQ	<LOQ
Contents in final Ag_3PO_4 precipitates (mg):						
TP	1.69 ± 0.33	0.59 ± 0.00	<LOQ	0.76 ± 0.04	1.48 ± 0.11	4.87 ± 0.41
As	0.12 ± 0.05	0.03 ± 0.00	<LOQ	0.03 ± 0.00	0.01 ±0.00	<LOQ
Fe	<LOQ	<LOQ	<LOQ	<LOQ	<LOQ	<LOQ
Si	<LOQ	<LOQ	<LOQ	<LOQ	<LOQ	<LOQ
As to P molar ratios $R_{As/P}$:						
(1) in groundwater	0.13	0.60	0.25	0.19	0.02	
(2) in final Ag_3PO_4 precipitates	0.03 ± 0.01	0.02 ± 0.01	-	0.02 ± 0.00	0.003 ± 0.000	
Possible influence of As on isotope composition $\Delta_{true\text{-}meas}$ [‰]	+0.73	+0.51		+0.39	+0.07	

Supplementary Material: $\delta^{18}O_{PO4}$ analysis

Methodological background: In contrast to other important nutrients such as nitrate, the lack of more than one stable isotope (^{31}P) prevented stable isotope investigations on P. Additionally, extensive and partly dangerous laboratory procedures for the preparation of oxygen isotope measurements of phosphate ($\delta^{18}O_{PO4}$) complicated the application except for paleoenvironmental investigations on apatite. Since the first study that determined the $^{18}O/^{16}O$ ratio in phosphates (Tudge 1960), several methodological modifications and improvements have been made to process environmental samples with various matrices for $\delta^{18}O_{PO4}$ analysis. These methods comprise often multiple co-precipitations, precipitations, and resin treatment steps with the aim of isolating, concentrating, purifying and quantitatively transferring PO_4^{3-} into the solid phase. The current state-of the art method to analyze $\delta^{18}O_{PO4}$ is by means of an isotope ratio mass spectrometer (IRMS) in form of pure and solid silver phosphate, Ag_3PO_4 (Crowson et al. 1991, Firsching 1961, Lécuyer 2004). Recent methodological protocols have then gradually been applied to trace potential sources, follow pathways and to gain insights into biological cycling of P in terrestric as well as aquatic environments as summarized in two extensive recent reviews (Davies et al. 2014, Tamburini et al. 2014).

Pilot study: Despite a steadily increasing amount of publications utilizing $\delta^{18}O_{PO4}$ analysis to address environmental questions, only very few groundwater studies included this novel approach so far (Blake et al. 2001, Davies 2016, McLaughlin et al. 2006, Young et al. 2009). High concentrations of PO_4^{3-} in groundwater render Asian aquifers as an ideal testing ground for this innovative method, but no suitable protocol exists so far for its extraction from anoxic groundwater and subsequent purification. Hence, we conducted a pilot study at our study site at Van Phuc aiming to (i) adapt existing methods for the analysis of $\delta^{18}O_{PO4}$ to the specific requirements of anoxic groundwater; (ii) to apply this isotope approach to gain insight into the biogeochemical cycling of P in aquifer systems. Sample processing and analysis for $\delta^{18}O_{PO4}$ was conducted according to the overview provided in Fig. S3, which was based on a combination and modification of existing protocols developed for surface waters and liquid extractions (Gruau et al. 2005, McLaughlin et al. 2004, Tamburini et al. 2010).

Sampling and analytical procedure: Five wells were selected for sampling in Van Phuc, of which four yielded sufficient P for the $\delta^{18}O_{PO4}$ analysis and were successfully processed to Ag_3PO_4. For each well duplicate samples of 1 L groundwater were collected in pre-cleaned, acid-washed and pre-conditioned 1.5 L PP bottles. Samples were then aerated for 24 hours to co-precipitate PO_4^{3-} with freshly formed Fe(III)-(hydr)oxides, originating from the high concentrations of dissolved Fe^{2+} in respective groundwater samples (0.71 to 16.1 mg L^{-1}). Dissolved Fe^{2+} immediately reacts with atmospheric O_2 resulting in oxidation and precipitation of Fe(III)-(hydr)oxides and co-precipitation of PO_4^{3-} (Hug et al. 2008, Senn et al. 2015, Voegelin et al. 2013). Sample acidification would prevent this reaction, but might cause hydrolysis of organic P (P_o). Hence, precipitation of Fe(III)-(hydr)oxides was applied in the field as a first step in order to isolate and pre-concentrate PO_4^{3-} from groundwater and interfering solutes (Gruau et al. 2005). The Fe-precipitates were separated from groundwater by vacuum filtration (0.2 µm cellulose filters, Roth), air-dried and then transported to our lab facilities in Tübingen for further processing.

The Fe(III)-(hydr)oxide precipitates were first dissolved in 40 mL of 16.5 % HNO_3 (Merck, p.a.) to liberate co-precipitated PO_4^{3-}. Remaining filters were additionally rinsed with 10 mL Millipore water to ensure a complete removal of PO_4^{3-}. Afterwards the protocol followed basically the published method from Tamburini et al. (2010) for soil extractions. Due to the lack of a commercial reference material an *in-house* standard (KH_2PO_4, Roth, p.a.) was included as quality control, which was exactly treated like the natural samples. The protocol included two further precipitation steps and a resin treatment step aiming at removing impurities to receive a clean final Ag_3PO_4-precipitate for the analysis by IRMS. First, PO_4^{3-} was precipitated in form of ammonium-phospho-molybdate (APM, $(NH_4)_3PMo_{12}O_{40}$) by adding 25 mL of 4.2 M NH_4NO_3 solution (Roth) in a water bath at 50 °C. Then, 40mL of 10% ammonium molybdate solution ($(NH_4)_6Mo_7O_{24}x4H_2O$) (Roth, 99%) was added and yellow APM crystals formed overnight during gentle stirring. These crystals were then collected by vacuum filtration with 0.2 µm cellulose acetate filters and rinsed several times with 0.6 M NH_4NO_3 solution. The APM precipitate was then dissolved by gently stirring the crystals in 50mL ammonium-citrate solution (Tamburini et al.

2010). The next precipitation step was then induced by adding 25 mL acidic magnesia solution (Tamburini et al. 2010) that was brought to a pH of 8 to 9 by the addition of about 7 mL of 1:1 NH_4OH/H_2O (v:v) solution. White magnesium ammonium phosphate crystals (MAP or struvite, $NH_4MgPO_4x6H_2O$) formed while stirring overnight. After separation by vacuum filtration, the struvite crystals were washed thoroughly with 1:20 NH_4OH/H_2O (v:v) solution. Struvite crystals were dissolved by adding about 20 mL of 0.5 M HNO_3. After dissolution, possible interfering cations were removed by shaking the samples together with 6mL of a cation exchange resin slurry (BioRad, AG® 50W-X8, analytical grade, 20–50 mesh, H+-form) overnight (McLaughlin et al. 2004, Tamburini et al. 2010). Resin and sample solution were separated by filtration onto 0.2 µm polycarbonate filters. The collected sample solution and approximately 2 mL of Millipore water (used to rinse the collected resin) were then transferred to new 50 mL tubes. The solution obtained was checked for the presence of interfering Cl^- remains by adding small amounts of $AgNO_3$ (McLaughlin et al. 2004). If AgCl still precipitated, the sample solution was filtered again after a few minutes. This step was repeated until no more precipitate formed to ensure that Cl^- removal was complete. Finally, PO_4^{3-} was precipitated as Ag_3PO_4 following the addition of 5 mL silver ammine solution (Tamburini et al. 2010) and placing the open tubes into an oven at 50°C for 48 hours. If no precipitate formed, the pH was checked and manually adjusted to pH 7 if required. The Ag_3PO_4 precipitate was collected on 0.2 µm polycarbonate filters and dried for a minimum of 24 hours at 50 °C. Triplicates (duplicates for samples with insufficient sample material) of 0.4-0.6 mg Ag_3PO_4 were weighed into Ag capsules (HekaTech) for the analysis by TC/EA-IRMS (HekaTech HTO; Isoprime GV IRMS). Four of the five sampled wells (AMS-5, AMS-11, VPNS-5 and VPNS-9) yielded sufficient Ag_3PO_4 for the analysis. While for sample VPNS-9 only one sample of the duplicates was successfully processed to the final stage, all other duplicate samples agree within the external reproducibility (Table S6). The IRMS measurements were calibrated using the international VSMOW ($\delta^{18}O$= 0.00 ± 0.30‰, n= 5) and GISP reference standard ($\delta^{18}O$= -24.76 ± 0.16‰, n= 4), and an *in-house* Ag_3PO_4 standard ($\delta^{18}O$= 20.68 ± 0.20‰, n= 14).

Method evaluation: While in groundwater different PO_4^{3-} sources and modifications of the respective isotope composition (i.e. via enzymatic turnover) contribute to the final measured $\delta^{18}O_{PO4}$ value, a further alteration of the isotopic signal must be prevented during the elaborate laboratory processing. The isotopic composition of the KH_2PO_4 laboratory standard that was processed together with the samples (13.51 ± 0.35 ‰, n=3) matched the composition of the unprocessed pure material (13.79 ± 0.25 ‰, n=8), indicating no alterations during the sample preparation. This is further in line with $\delta^{18}O_{PO4}$ values reported for KH_2PO_4 before and after treatment elsewhere (Chang and Blake 2015). We additionally monitored TDP concentrations in solutions of different processing steps to prevent possible fractionations due to an incomplete transfer of PO_4^{3-}. Also, solutions were analyzed regarding potential contaminations with other oxygen-bearing compounds (e.g., As). Therefore, 0.5 mL aliquots were collected from sample solutions and the KH_2PO_4 laboratory standard (concentration: 5 mg L^{-1}), and 10 mL from supernatants (after the precipitation of AMP, struvite and Ag_3PO_4, respectively), see Table S7. Samples were analyzed by ICP-OES (Optima 5300 DV, Perkin Elmer) for TDP (wavelength λ: 214.914 axial, detection limit dl: 0.006 mg L^{-1}; except for samples with high Mo concentrations after the APM precipitation, here λ:178.221 axial, dl: 0.051 mg L^{-1}).

Supernatants after specific precipitation steps did not show any detectable TDP concentrations, reflecting a successful quantitative precipitation of PO_4^{3-} from the solutions (Table S7). Furthermore, solutions after respective dissolution steps showed the expected amount of TDP, pointing to a complete transfer from the initial Fe(III)-(hydr)oxides to the final Ag_3PO_4 precipitate. Additionally, speciation investigation revealed that PO_4^{3-} constituted the dominant P species in groundwater at Van Phuc (see chapter 3.1), excluding the possibility that hydrolysis of P_o occurred during sample processing. Results from the ICP-OES also indicated that except for As, a transfer of other oxyanion-forming elements (e.g. Mo, V) into the final Ag_3PO_4 precipitate was insignificant since respective concentrations in groundwater and solutions remained in the low ppm to ppb range.

To account for the potential influence of As-bound oxygen on the $\delta^{18}O_{PO4}$ signal in the Ag_3PO_4 precipitate, a simple two-endmember mixing model was applied. The measured $\delta^{18}O_{Pmeas}$ value was therefore assumed to be a combination of the isotopic composition of "true" Ag_3PO_4 and co-precipitated Ag_3AsO_4. Since Ag_3AsO_4 was shown to readily exchange its oxygen with ambient H_2O

(Tang 2014)), the oxygen isotope composition of potentially present As ($\delta^{18}O_{As}$) was assumed to be equivalent to the isotopic composition of our laboratory water ($\delta^{18}O_{Wlab}$= -8.86 ± 0.07 ‰, determined for a blank solution from the final Ag_3PO_4 precipitation step). The As content in the final precipitates was determined for all samples by measuring the As content in solution before and after precipitation of Ag_3PO_4. With this, the As to P molar ratio ($R_{As/P}$) in the precipitates (Table S7) was calculated and the oxygen isotope composition of a pure Ag_3PO_4 ($\delta^{18}O_{Ptrue}$) was extrapolated via

$$\delta^{18}O_{Ptrue} = \frac{R_{As/P}}{1 - R_{As/P}} * (\delta^{18}O_{Pmeas} - \delta^{18}O_{Wlab}) + \delta^{18}O_{Pmeas} \quad (S1)$$

with the difference between true and measured value calculated via

$$\Delta_{true-meas} = \delta^{18}O_{Ptrue} - \delta^{18}O_{Pmeas} \quad (S2)$$

as summarized in Table S7. The presence of As in the Ag_3PO_4 precipitate results in a potential shift to lighter apparent $\delta^{18}O_{PO4}$ values due to the mixture with isotopically light $\delta^{18}O_{Wlab}$. Depending on the As content, this shift could range from +0.07 to +0.73 ‰ in our samples.

Supplementary Material: Literature

Al Lawati, W.M., Rizoulis, A., Eiche, E., Boothman, C., Polya, D.A., Lloyd, J.R., Berg, M., Vasquez-Aguilar, P.,van Dongen, B.E., 2012. Characterisation of organic matter and microbial communities in contrasting arsenic-rich Holocene and arsenic-poor Pleistocene aquifers, Red River Delta, Vietnam. Appl. Geochem. 27, 315-325.

Biswas, A., Neidhardt, H., Kundu, A.K., Halder, D., Chatterjee, D., Berner, Z., Jacks, G.,Bhattacharya, P., 2014. Spatial, vertical and temporal variation of arsenic in shallow aquifers of the Bengal Basin: Controlling geochemical processes. Chem. Geol. 387, 157-169.

Blake, R.E., Alt, J.C.,Martini, A.M., 2001. Oxygen isotope ratios of PO4: An inorganic indicator of enzymatic activity and P metabolism and a new biomarker in the search for life. Proc. Natl. Acad. Sci. USA 98, 2148-2153.

Chang, S.J.,Blake, R.E., 2015. Precise calibration of equilibrium oxygen isotope fractionations between dissolved phosphate and water from 3 to 37 °C. Geochim. Cosmochim. Acta 150, 314-329.

Crowson, R.A., Showers, W.J., Wright, E.K.,Hoering, T.C., 1991. Preparation of phosphate samples for oxygen isotope analysis. Analytical Chemistry 63, 2397-2400.

Davies, C., 2016. Developing a stable isotope approach to trace the sources and metabolism of phosphorus in freshwaters, PhD thesis, Lancaster University.

Davies, C.L., Surridge, B.W.J.,Gooddy, D.C., 2014. Phosphate oxygen isotopes within aquatic ecosystems: Global data synthesis and future research priorities. Sci. Total Environ. 496, 563-575.

Eiche, E., Neumann, T., Berg, M., Weinman, B., van Geen, A., Norra, S., Berner, Z., Trang, P.T.K., Viet, P.H.,Stüben, D., 2008. Geochemical processes underlying a sharp contrast in groundwater arsenic concentrations in a village on the Red River delta, Vietnam. Appl. Geochem. 23, 3143-3154.

Firsching, F.H., 1961. Precipitation of Silver Phosphate from Homogenous Solution. Analytical Chemistry 33, 873-874.

Gruau, G., Legeas, M., Riou, C., Gallacier, E., Martineau, F.,Hénin, O., 2005. The oxygen isotope composition of dissolved anthropogenic phosphates: a new tool for eutrophication research? Water Res. 39, 232-238.

Hug, S.J., Leupin, O.X.,Berg, M., 2008. Bangladesh and Vietnam: Different Groundwater Compositions Require Different Approaches to Arsenic Mitigation. Environ. Sci. Technol. 42, 6318-6323.

Lécuyer, C., 2004. Chapter 22 - Oxygen Isotope Analysis of Phosphate A2 - Groot, Pier A. de. In, Handbook of Stable Isotope Analytical Techniques. Elsevier, Amsterdam, pp. 482-496.

311 Longinelli, A.,Nuti, S., 1973. Revised phosphate-water isotopic temperature scale. Earth Planet. Sc.
312 Lett. 19, 373-376.
313 McLaughlin, K., Cade-Menun, B.J.,Paytan, A., 2006. The oxygen isotopic composition of phosphate in
314 Elkhorn Slough, California: A tracer for phosphate sources. Estuar. Coast. Shelf Sci. 70, 499-506.
315 McLaughlin, K., Silva, S., Kendall, C., Stuart-Williams, H.,Paytan, A., 2004. A precise method for the
316 analysis of δ18O of dissolved inorganic phosphate in seawater. Limnol. Oceanogr. Methods 2, 202-
317 212.
318 Neidhardt, H., Berner, Z., Freikowski, D., Biswas, A., Winter, J., Chatterjee, D.,Norra, S., 2013.
319 Influences of groundwater extraction on the distribution of dissolved As in shallow aquifers of West
320 Bengal, India. J. Hazard. Mater. 262, 941-950.
321 Neidhardt, H., Berner, Z.A., Freikowski, D., Biswas, A., Majumder, S., Winter, J., Gallert, C., Chatterjee,
322 D.,Norra, S., 2014. Organic carbon induced mobilization of iron and manganese in a West Bengal
323 aquifer and the muted response of groundwater arsenic concentrations. Chem. Geol. 367, 51-62.
324 Neidhardt, H., Winkel, L.H.E., Kaegi, R., Stengel, C., Trang, P.T.K., Lan, V.M., Viet, P.H.,Berg, M., 2018.
325 Insights into arsenic retention dynamics of Pleistocene aquifer sediments by in situ sorption
326 experiments. Water Res. 129, 123-132.
327 Senn, A.-C., Kaegi, R., Hug, S.J., Hering, J.G., Mangold, S.,Voegelin, A., 2015. Composition and
328 structure of Fe(III)-precipitates formed by Fe(II) oxidation in water at near-neutral pH:
329 Interdependent effects of phosphate, silicate and Ca. Geochim. Cosmochim. Acta 162, 220-246.
330 Tamburini, F., Bernasconi, S.M., Angert, A., Weiner, T.,Frossard, E., 2010. A method for the analysis of
331 the δ18O of inorganic phosphate extracted from soils with HCl. Eur. J. Soil Sci. 61, 1025-1032.
332 Tamburini, F., Pfahler, V., von Sperber, C., Frossard, E.,Bernasconi, S.M., 2014. Oxygen Isotopes for
333 Unraveling Phosphorus Transformations in the Soil–Plant System: A Review. Soil Sci. Soc. Am. J. 78,
334 38-46.
335 Tang, X., 2014. Separating arsenic oxyanions from natural waters for oxygen isotope analysis, PhD
336 thesis, KIT Scientific Publishing.
337 Tudge, A., 1960. A method of analysis of oxygen isotopes in orthophosphate—its use in the
338 measurement of paleotemperatures. Geochim. Cosmochim. Acta 18, 81-93.
339 van Geen, A., Bostick, B.C., Thi Kim Trang, P., Lan, V.M., Mai, N.-N., Manh, P.D., Viet, P.H., Radloff, K.,
340 Aziz, Z., Mey, J.L., Stahl, M.O., Harvey, C.F., Oates, P., Weinman, B., Stengel, C., Frei, F., Kipfer,
341 R.,Berg, M., 2013. Retardation of arsenic transport through a Pleistocene aquifer. Nature 501, 204-
342 207.
343 Voegelin, A., Senn, A.-C., Kaegi, R., Hug, S.J.,Mangold, S., 2013. Dynamic Fe-precipitate formation
344 induced by Fe(II) oxidation in aerated phosphate-containing water. Geochim. Cosmochim. Acta 117,
345 216-231.
346 Weinman, B., Goodbred, S., Savage, K., Zheng, Y., Radloff, K., Singhvi, A., Charlet, L., Berg, M., Eiche,
347 E.,Cribb, W. 2008. The Co-Evolution of Asian Aquifers and Arsenic: How Understanding Sedimentary
348 History can Help Predict Patterns of Arsenic Heterogeneity. AGU Fall Meeting Abstracts, Abstr. H52B-
349 04.
350 Young, M.B., McLaughlin, K., Kendall, C., Stringfellow, W., Rollog, M., Elsbury, K., Donald, E.,Paytan,
351 A., 2009. Characterizing the Oxygen Isotopic Composition of Phosphate Sources to Aquatic
352 Ecosystems. Environ. Sci. Technol. 43, 5190-5196.

353